Studies on Blue Copper Protein Models: Syntheses, Properties, and Electron-transfer Reactions of Bis[4-(alkylmercaptomethyl)imidazole]-copper(II) Diperchlorate and Related Complexes and *X*-Ray Crystallographic Analysis of Bis[4-(n-propylmercaptomethyl)imidazole-*N*^{3}*S*]copper(II) Diperchlorate †

Nobuo Aoi, Gen-etsu Matsubayashi, and Toshio Tanaka *
Department of Applied Chemistry, Faculty of Engineering, Osaka University, Yamada-oka, Suita, Osaka 565, Japan

---

Bis[4-(alkyl- and bis[4-(phenyl-mercaptomethyl)imidazole]copper(II) diperchlorates (alkyl = n-propyl, t-butyl, or benzyl) and 1,6-bis(imidazol-4′-yl)-2,5-dithiahexanecopper(II) diperchlorate were prepared. The cationic moieties of these complexes undergo electrochemically reversible redox reactions at the potentials $E_{\frac{1}{2}}$ = +0.23 to +0.36 V *vs.* s.c.e. in methanol containing [NBu$^n_4$][BF$_4$] (0.1 mol dm^{-3}) as a supporting electrolyte. Kinetic studies on the reductions of these complexes with ferrocene in methanol reveal that precursor complexes are formed prior to electron transfer between the reactants; the formation constants of the precursor complexes are in the range 9.7—32.2 dm^3 mol^{-1}. The activation entropies for the electron-transfer reaction were obtained as positive values, +33 to +71 J K^{-1} mol^{-1}, which suggests that the precursor complex undergoes desolvation in a transition state. Electronic absorption and e.s.r. spectra of the copper(II) complexes as well as the *X*-ray crystal structure of bis[4-(n-propylmercaptomethyl)imidazole]copper(II) diperchlorate are described. The *X*-ray crystal structure shows the copper to be centrosymmetrically co-ordinated by two thioether sulphur atoms [Cu–S 2.397(2) Å], two imidazole nitrogen atoms [Cu–N 1.940(6) Å], and two oxygen atoms from unidentate perchlorate ions [Cu–O 2.594(6) Å].

Blue (type I) copper proteins exhibit unusual spectral and electrochemical properties in comparison with those of common copper(II) complexes; the proteins exhibit intense absorption bands near 600 nm (ε = 3 500—11 300 dm^3 mol^{-1} cm^{-1}), small electron–copper nuclear hyperfine coupling constants ($A_{\parallel}$ = 31 × 10^{-4} to 90 × 10^{-4} cm^{-1}), and relatively high Cu^{II}–Cu^{I} redox potentials ($E_{\frac{1}{2}}$ = 0 to +0.6 V *vs.* s.c.e.).[1] Recent single-crystal *X*-ray diffraction studies on Cu^{II} *Poplar* plastocyanin and *Pseudomonas aeruginosa azurin* have demonstrated that the copper(II) ion as an active site is placed in a distorted tetrahedral geometry formed by two imidazole nitrogen atoms of histidine residues and two sulphur atoms of cysteinate thiolate and methionine thioether.[2] Although the biological roles of blue copper proteins are not yet fully understood, plastocyanin is thought to function as an electron-transport sequence in photosynthetic organisms with the aid of interconversion between Cu^{II} and Cu^{I} states.[1] To date, several complexes involving the CuS$_2$N$_2$ core as models for the active site of blue copper proteins have been synthesized and characterized,[3-10] although little is known about copper(II) complexes involving both imidazole nitrogen and thioether sulphur as ligating atoms.‡ In addition, kinetic studies have been reported on electron-transfer reactions between Cu^{II}S$_2$N$_2$ complexes and cytochrome c.[11] The present study was undertaken to bring about a further understanding of blue copper proteins.

This paper reports the preparation, spectroscopic, and electrochemical properties of bis[4-(alkyl- and bis[4-(phenyl-mercaptomethyl)imidazole]copper(II) diperchlorates (1)—(4) and 1,6-bis(imidazol-4′-yl)-2,5-dithiahexanecopper(II) diperchlorate (5), together with the *X*-ray crystal structure of bis[4-(n-propylmercaptomethyl)imidazole]copper(II) diperchlorate (1). Moreover, the kinetics of the redox reaction of these copper(II) complexes with ferrocene are described.

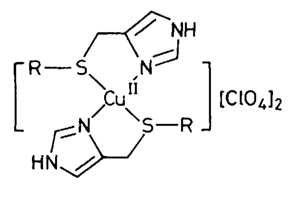

[Cu(L^1)$_2$][ClO$_4$]$_2$ (1; R = Pr^n)
[Cu(L^2)$_2$][ClO$_4$]$_2$ (2; R = Bu^t)
[Cu(L^3)$_2$][ClO$_4$]$_2$ (3; R = CH$_2$Ph)
[Cu(L^4)$_2$][ClO$_4$]$_2$ (4; R = Ph)

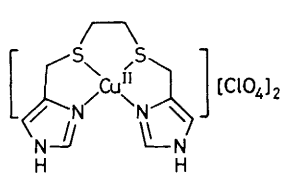

[CuL^5][ClO$_4$]$_2$ (5)

Experimental

Materials.—4-(Alkyl- and 4-(phenyl-mercaptomethyl)imidazole hydrochlorides (alkyl = Pr^n, Bu^t, or CH$_2$Ph) and 1,6-bis(imidazol-4′-yl)-2,5-dithiahexane dihydrochloride were prepared according to the literature methods.[12] To aqueous solutions of these hydrochlorides were added dropwise large excess amounts of aqueous ammonia to give white suspensions which were extracted with 1,2-dichloroethane. The extracts were evaporated under reduced pressure to give oil-free bases of the mercaptomethylimidazole derivatives. They were characterized by ^{1}H n.m.r. spectroscopy and used for preparations of the copper(II) complexes.

Commercially available ferrocene was purified by sublimation before use in the redox reaction with the copper(II) complexes.

Deionized water was used in preparations of the ligands.

---

† *Supplementary data available* (No. SUP 23552, 8 pp.): structure factors, thermal parameters. See Notices to Authors No. 7, *J. Chem. Soc., Dalton Trans.*, 1981, Index issue.

Non-S.I. unit employed: G = 10^{-4} T.

‡ The Cu^{II} complex of cimetidine is only known as such, although the Cu^{II} ion is placed in an octahedral geometry formed by two S and four N atoms as determined by the *X*-ray analysis.[8]

Table 1. Colours, yields, and analytical data of the copper complexes

Complex	Colour	Yield (%)	Analysis [a] (%) C	H	N
(1)	Brown plates	57	28.95	4.15	9.55
			(29.25)	(4.2)	(9.75)
(2)	Brown microcrystals	30	31.7	4.75	9.6
			(31.9)	(4.7)	(9.3)
(3)	Brown plates	15	39.4	3.6	8.35
			(39.25)	(3.7)	(8.4)
(4) [b]	Purple microcrystals	15	36.3	3.4	8.55
			(36.35)	(3.35)	(8.5)
(5) [b]	Light green needles	25	22.1	3.2	10.35
			(22.45)	(3.0)	(10.45)

[a] Calculated values in parentheses. [b] Isolated as monohydrates.

1,2-Dichloroethane was purified in the usual manner.[13] Methanol and ethanol were distilled with sodium alkoxide.

Preparations of Bis[4-(*alkyl- and Bis*[4-(*phenyl-mercaptomethyl*)*imidazole*]*copper*(II) *Diperchlorates*, $[Cu(L)_2][ClO_4]_2$ [R = Pr^n (1), Bu^t (2), CH_2Ph (3), *or* Ph (4)], *and* 1,6-*Bis*-(*imidazol*-4′-*yl*)-2,5-*dithiahexanecopper*(II) *Diperchlorate*, $[CuL^5][ClO_4]_2$ (5).—To an ethanol (5 cm^3) solution of 4-(n-propylmercaptomethyl)imidazole (L^1) (0.50 g, 3.2 mmol) was added $Cu(ClO_4)_2{\cdot}6H_2O$ (0.59 g, 1.6 mmol) dissolved in the same solvent (5 cm^3). The resulting deep green solution was allowed to stand overnight at room temperature, giving a precipitate, which was collected by filtration and recrystallized from methanol–ethanol (1 : 1 v/v) to yield brown plates of (1). Other copper(II) complexes (2)—(5) were prepared similarly by the reaction of $Cu(ClO_4)_2{\cdot}6H_2O$ with the corresponding imidazole. Properties and analytical data of these copper(II) complexes obtained are summarized in Table 1. No melting points could be determined, due to the explosive nature of the complexes.

Physical Measurements.—Electronic absorption spectra were obtained using a Union SM-401 spectrophotometer. Electron spin resonance spectra were recorded on a JEOL ME-2X spectrometer and were calibrated with diphenylpicrylhydrazyl (g = 2.0037). Cyclic voltammetry was performed in a conventional cell consisting of a platinum disc as a working electrode, a platinum plate (2 × 2 cm) as a counter electrode, and a saturated calomel reference electrode (s.c.e.), using $[NBu^n{}_4][BF_4]$ or $[NBu^n{}_4][ClO_4]$ as a supporting electrolyte.

Kinetic measurements were carried out in methanol under a nitrogen atmosphere under pseudo-first-order conditions with at least 10-fold excess amounts of ferrocene over the copper(II) complexes (3×10^{-4} to 4×10^{-4} mol dm^{-3}), except that for the reaction of (5) with ferrocene in which at least 100-fold excess amounts of ferrocene were used, since the reaction is thermodynamically unfavourable. The reaction rates were determined by monitoring the decay or rise of absorption bands at 270—400 nm using a Union RA-103 stopped-flow spectrophotometer equipped with a 2-mm quartz cell in a cell-holder thermostatted within ±0.2 °C.

X-*Ray Crystal Structure Analysis.*—A single crystal of (1) with approximate dimensions 0.06 × 0.10 × 0.22 mm was selected for *X*-ray diffraction studies and was mounted approximately along the longest dimension. The space group and initial unit-cell parameters were determined from oscillation and Weissenberg photographs. Accurate cell constants were determined by the least-squares refinement of the angular settings of 45 reflections with 2θ values up to 27°.

Table 2. Atomic co-ordinates ($\times 10^4$; H, $\times 10^3$) for $[Cu(L^1)_2]$-$[ClO_4]_2$ (1; R = Pr^n) with estimated standard deviations in parentheses

Atom	x	y	z
Cu	0(0)	0(0)	0(0)
Cl	513(2)	−1 555(2)	−2 585(1)
S	−2 327(2)	523(2)	13(1)
O(1)	165(6)	−1 734(8)	−1 574(4)
O(2)	−617(7)	−1 027(9)	−3 110(5)
O(3)	1 549(7)	−412(8)	−2 694(6)
O(4)	916(6)	−3 115(7)	−2 954(4)
N(1)	96(6)	2 050(8)	−679(4)
N(2)	613(7)	4 115(8)	−1 597(5)
C(1)	1 046(7)	2 693(9)	−1 231(5)
C(2)	−659(8)	4 370(10)	−1 279(6)
C(3)	−955(7)	3 122(9)	−696(5)
C(4)	−2 156(8)	2 704(9)	−151(6)
C(5)	−2 875(7)	−93(11)	−1 200(6)
C(6)	−3 163(9)	−1 902(11)	−1 217(7)
C(7)	−4 413(11)	−2 338(14)	−649(8)
HC(1)	186(7)	232(9)	−143(5)
HC(2)	−107(9)	520(10)	−135(6)
HN(2)	107(9)	459(11)	−194(6)
HC(41)	−309(9)	309(11)	−51(6)
HC(42)	−207(6)	320(8)	52(5)
HC(51)	−356(9)	61(11)	−124(6)
HC(52)	−230(9)	11(11)	−154(6)
HC(61)	−255(9)	−253(11)	−90(6)
HC(62)	−329(10)	−231(12)	−180(7)

Crystal data. $C_{14}H_{24}Cl_2CuN_4O_8S_2$ (1), M = 574.9, Monoclinic, space group $P2_1/n$, a = 10.131(1), b = 8.229(1), c = 13.663(1) Å, β = 90.40(1)°, U = 1 139.1(3) Å^3, Z = 2, D_c = 1.676(1) g cm^{-3}, $F(000)$ = 590, μ(Mo-K_α) = 14.5 cm^{-1}.

Intensity data were collected on an automated Rigaku four-circle diffractometer for all reflections in the range 20—55° and with $k > 0$ and $l > 0$ by using graphite-monochromatized Mo-K_α (λ = 0.710 69 Å) radiation. The ω—2θ scan mode was used with a 2θ scan rate of 2° min^{-1}. The scan width in 2θ was $(1.0 + 0.34 \tan\theta)°$, and 60-s background counts were taken on either side of each scan. Five check reflections were monitored before every 50 reflections. There was no significant change in their intensities during the data collection. The intensities were corrected for Lorentz and polarization effects. No correction was made for absorption. Of the 2 619 independent reflections, 1 534 had structure amplitudes larger than three times their standard deviations. They were used in the subsequent calculations.

Structure determination. The positions of the copper and sulphur atoms were indicated on a three-dimensional Patterson map. Subsequent cycles of Fourier syntheses and block-diagonal least-squares calculations gave a reasonable set of co-ordinates and thermal parameters for all the non-hydrogen atoms. A difference-Fourier map based on the anisotropic refinement showed electron densities in positions which were attributed to imidazole ring- and methylene-hydrogen atoms. The methyl hydrogen atoms, however, were omitted from the refinement because their positions could not be determined with any certainty. In the final four cycles of the block-diagonal least-squares refinement with anisotropic thermal parameters for all the non-hydrogen atoms and with isotropic thermal parameters for hydrogen atoms, the residual indices were $R = \Sigma||F_o| - |F_c||/\Sigma|F_o| = 0.066$ and $R' = [\Sigma w(|F_o| - |F_c|)^2/\Sigma w|F_o|^2]^{\frac{1}{2}} = 0.078$. The weighting scheme, $1/w = \sigma^2(F_o) + 0.001(F_o)^2$, was used. The final difference-Fourier map had no

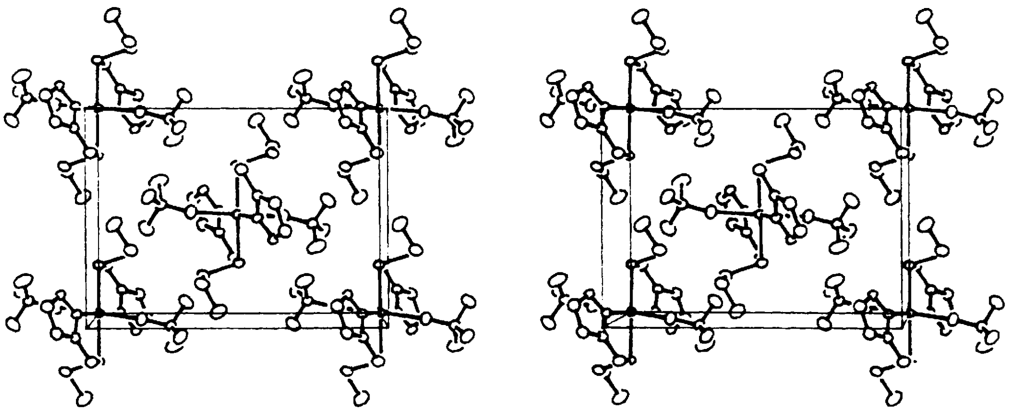

Figure 1. Stereoscopic packing diagram for $[Cu(L^1)_2][ClO_4]_2$ (1). The origin of the cell is at the bottom left corner. The z axis is horizontal, the x axis is vertical, and the y axis points out from the origin

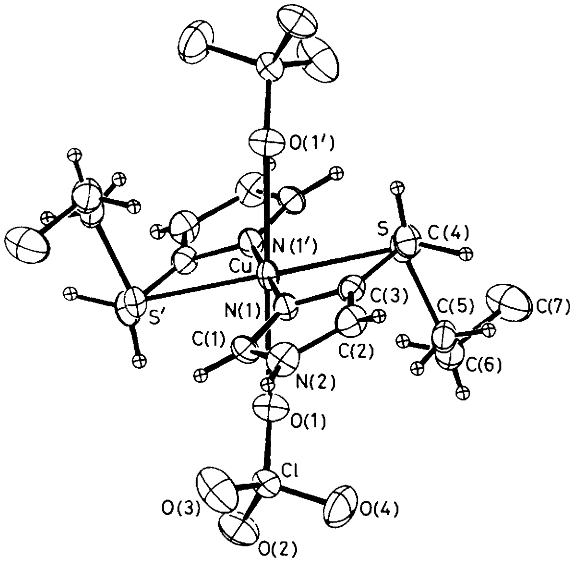

Figure 2. Molecular structure of $[Cu(L^1)_2][ClO_4]_2$ (1) with the atom labelling scheme

positive maxima >1 e Å^{-3} except in the vicinity of the methyl carbon and copper atoms. Atomic scattering factors for Cu^{2+}, Cl^-, and neutral S, C, N, O, and H were taken from ref. 14 as were the anomalous dispersion corrections for Cu^{2+}, Cl^-, and S. Final atomic co-ordinates are given in Table 2.

Crystallographic calculations were performed on an ACOS 700S computer at the Crystallographic Research Centre, Institute for Protein Research, Osaka University. Figures 1 and 2 were drawn on a NUMERICON 7000 system at the Crystallographic Research Centre with local version of ORTEP-II.[15]

Table 3. Selected bond distances and angles for $[Cu(L^1)_2][ClO_4]_2$ (1; R = Pr^n) with estimated standard deviations in parentheses

(*a*) Bond distances (Å)

Cu–S	2.397(2)	C(2)–C(3)	1.342(11)
Cu–O(1)	2.594(6)	C(3)–C(4)	1.473(11)
Cu–N(1)	1.940(6)	C(5)–C(6)	1.529(13)
S–C(4)	1.832(8)	C(6)–C(7)	1.534(11)
S–C(5)	1.818(8)	Cl–O(1)	1.436(6)
N(1)–C(1)	1.338(9)	Cl–O(2)	1.416(7)
N(1)–C(3)	1.387(9)	Cl–O(3)	1.423(7)
N(2)–C(1)	1.354(10)	Cl–O(4)	1.449(6)
N(2)–C(2)	1.379(11)		

(*b*) Bond angles (°)

S–Cu–O(1)	100.1(1)	Cu–N(1)–C(1)	131.1(5)
S–Cu–N(1)	84.1(2)	Cu–N(1)–C(3)	121.9(5)
O(1)–Cu–N(1)	95.0(2)	C(1)–N(1)–C(3)	106.8(6)
O(1)–Cl–O(2)	108.4(4)	C(1)–N(2)–C(2)	108.6(7)
O(1)–Cl–O(3)	110.8(4)	N(1)–C(1)–N(2)	108.9(6)
O(1)–Cl–O(4)	108.3(4)	N(2)–C(2)–C(3)	106.4(7)
O(2)–Cl–O(3)	109.6(4)	N(1)–C(3)–C(2)	109.3(7)
O(2)–Cl–O(4)	109.2(4)	N(1)–C(3)–C(4)	118.5(6)
O(3)–Cl–O(4)	110.5(4)	C(2)–C(3)–C(4)	132.1(7)
Cu–S–C(4)	94.8(3)	S–C(4)–C(3)	111.9(5)
Cu–S–C(5)	103.6(3)	S–C(5)–C(6)	110.4(6)
C(4)–S–C(5)	101.2(4)	C(5)–C(6)–C(7)	112.5(8)
Cu–O(1)–Cl	139.3(4)		

Results and Discussion

Description of the Structure of $[Cu(L^1)_2][ClO_4]_2$ (1; R = Pr^n). —A stereoview of the crystal structure of complex (1) is given in Figure 1. The structure consists of two discrete centrosymmetric molecules in a unit cell. Figure 2 shows the molecular geometry of (1) with the atom labelling scheme. Relevant bond distances and angles are summarized in Table 3. The imidazole nitrogen and the sulphur atoms of the ligand are co-ordinated to the copper(II) ion to form a strict CuS_2N_2 plane, where the two sulphur atoms as well as the two nitrogen atoms are located in *trans* positions to each other. Perchlorate oxygen atoms are co-ordinated to the copper(II) ion in apical positions. The geometry around the copper(II) ion is analogous to that of bis(β-methylmercaptoethylamine)copper(II) diperchlorate.[3] The Cu–S bond length [2.397(2) Å] of (1) is significantly longer than the sum (2.34 Å) of the in-plane radius of copper(II) ion (1.30 Å) [16] and the tetrahedral covalent radius of sulphur (1.04 Å).[17] Similar large Cu–S distances have been reported for some copper(II) complexes with thioether ligands, for example, bis(2,5-dithiahexane)copper(II) diperchlorate [2.354(1) Å; while another Cu–S distance is 2.320(1) Å],[18] bis(β-methylmercaptoethylamine)copper(II) diperchlorate [2.366(1) Å],[3] and bis[2-(ethylthio)ethyl]amine(2-pyridylmethyl)copper(II) sulphate [2.385(1) and 2.461(2) Å].[4] On the other hand, the Cu–N bond length [1.940(6) Å] of (1) is somewhat shorter than those of some copper(II) complexes with imidazole ligands, for example, tetrakis(imidazole)copper(II) diiodide [1.98(3) and 2.04(3) Å],[19] tetrakis(imidazole)copper(II)

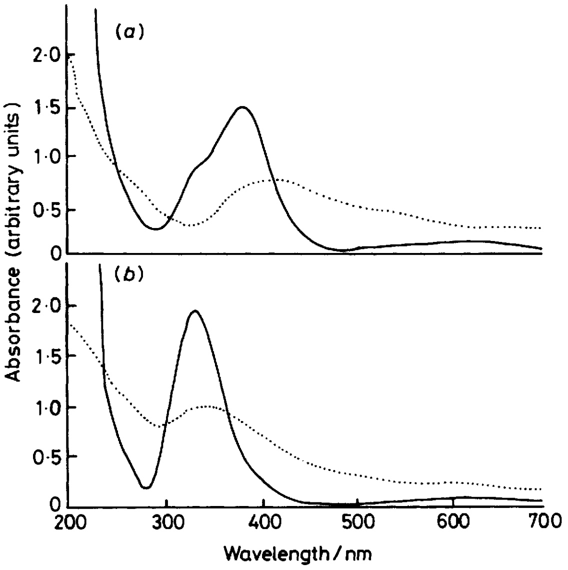

Figure 3. Electronic absorption spectra of $[Cu(L^1)_2][ClO_4]_2$ (1) (*a*), and $[CuL^5][ClO_4]_2$ (5) (*b*) in methanol–ethanol (1 : 4 v/v) (——), and in Nujol mulls (· · · · · ·)

sulphate [2.000(5) and 2.021(5) Å],[20] bis[2,2-bis(5′-phenylimidazol-2′-yl)propane]copper(II) diperchlorate [1.979(5) and 1.960(4) Å],[21] and bis[1,3-bis(5′-phenylimidazol-2′-yl)-2-thiapropane]copper(II) diperchlorate [2.019(7) and 2.020(9) Å].[21] Both perchlorate ions placed in the apical positions are weakly bonded to the copper(II) ion, as depicted by rather large Cu–O distances [2.594(6) Å] observed in complex (1). Similar large Cu–O bond lengths have been reported for bis(β-methylmercaptoethylamine)copper(II) diperchlorate [2.599(2) Å][3] and various $[CuL'][ClO_4]_2$ complexes (where L′ = ligand with N_4, S_2N_2, or S_4 centres; 2.53—2.68 Å).[3,5,22-24]

Electronic Absorption and E.S.R. Spectra, and Redox Behaviour.—Figure 3(*a*) and (*b*) show the electronic absorption spectra of (1) and (5), respectively, in both methanol–ethanol (1 : 4 v/v) and in the solid state. Intense bands observed in the solution spectra [$\lambda_{max.}$ = 382 nm for (1) and 334 nm for (5)] may be assigned to sulphur–copper charge-transfer (c.t.) transitions, since complexes with the $Cu^{II}S_2N_2$ skeleton, where S and N are thioether sulphur and amino- or pyridyl-nitrogen respectively, exhibit strong bands in the range 300—400 nm,[6,7] while the $Cu^{II}N_4$ type complexes involving only imidazole as ligands display no strong band in this region.[7] As described in the previous section, the *X*-ray structure analysis of (1) has revealed that the two sulphur atoms as well as the two nitrogen atoms are located in *trans* positions to each other. In addition, the solid-state spectra of (1) as well as (5) show low-energy shifts of the sulphur–copper c.t. bands accompanied by broadening compared with the solution spectra [Figure 3(*a*) and (*b*)]. Complex (1) in solution affords an additional band as a shoulder around 330 nm. This shoulder is tentatively assigned to the *cis* isomer with respect to two thioether sulphur atoms as well as two imidazole nitrogen atoms, because the shoulder is close in position to the absorption band of (5), whose geometry should be a *cis* configuration with respect to the two nitrogen atoms owing to the steric requirements of the ligand (L^5). Thus, the band at 382 nm observed in the solution spectrum of (1) may be assigned to the *trans* isomer.

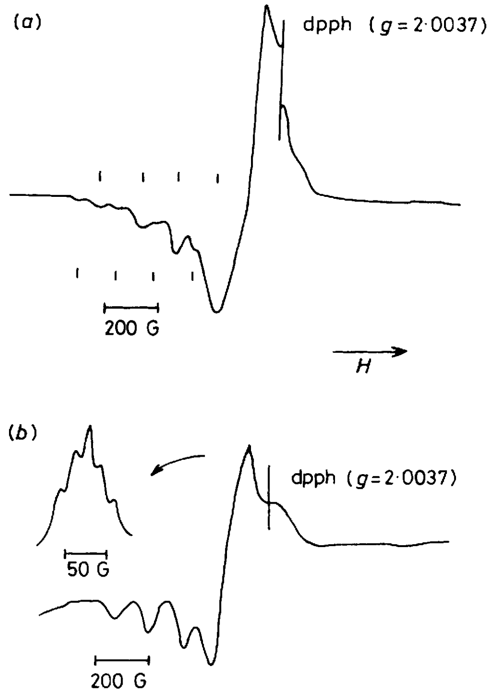

Figure 4. *X*-Band e.s.r. spectra of $[Cu(L^1)_2][ClO_4]_2$ (1) (*a*) and $[CuL^5][ClO_4]_2$ (5) (*b*) in methanol–ethanol (1 : 4 v/v) at 77 K (dpph = diphenylpicrylhydrazyl)

The co-existence of the *trans* and *cis* isomers of (1) is supported also from the e.s.r. spectrum in methanol–ethanol (1 : 4 v/v) at 77 K. This shows eight signals consisting of four intense and four weak ones in the $g_{\parallel}$ region arising from splitting due to the $^{63/65}Cu$ nuclei ($I = \frac{3}{2}$), as shown in Figure 4(*a*), while (5) exhibits only four e.s.r. signals in the same region, as seen in Figure 4(*b*). Complexes (2) and (3) exhibited e.s.r. spectra very similar to (1), whereas in the spectrum of (4) the signals due to the *trans* and *cis* isomers have not been well resolved. On the other hand, the spectrum of (5) shows super-hyperfine splittings ($A_{\perp}^{N}$ = 15 G) due to the two imidazole ^{14}N nuclei in the $g_{\perp}$ region, indicating the ligation of two imidazole nitrogen atoms to the copper(II) ion in (5).

The electronic absorption bands observed at shorter wavelengths than 300 nm in (1) and (5) are presumably derived from a nitrogen–copper c.t. transition and from a $\pi \longrightarrow \pi^*$ transition of the ligands, since $Cu^{II}N_4$ complexes containing amine and pyridine ligands have been reported to exhibit strong absorption bands due to a nitrogen–copper c.t. transition in the 200—300 nm region,[6,7] and the free L^1 (R = Pr^n) and L^5 molecules also displayed absorption bands in this region. The appearance of the spectra of (2) and (3) resembles well that of (1), while the spectrum of (4) is similar to that of (5). All the complexes in solution exhibited a weak broad band near 600 nm assignable to *d–d* transitions. This is in marked contrast to blue copper proteins having thiolate sulphur atoms which display an intense band in this region.[1] The electronic absorption maxima for complexes (1)—(5) are listed in Table 4 and the e.s.r. parameters of (1)—(5) are summarized in Table 5.

The $g_{\parallel}$ (2.24—2.29) and $g_{\perp}$ (2.07—2.09) values of these complexes are larger than those of complexes not only of the $Cu^{II}S_2N_2$ type, where S and N are thioether sulphur and amino- or pyridyl-nitrogen respectively {$g_{\parallel}$ = 2.12, $g_{\perp}$ = 2.05 for 2,10-diamino-4,8-dithiaundecanecopper(II) diperchlorate;[9] $g_{\parallel}$ = 2.16, $g_{\perp}$ = 2.05 for 1,8-bis(2′-pyridyl)-3,6-dithiaoctanecopper(II) diperchlorate;[9] $g_{\parallel}$ = 2.21 for [2-(2′-pyridyl)ethyl]bis[2-(ethylthio)ethyl]aminecopper(II) cation[25]}, but

Table 4. Electronic absorption bands ($\lambda_{max.}$/nm) of the copper(II) complexes at 25 °C

Complex	d–d [a]	Cu←S c.t. [a]	Cu←S c.t. [b]
(1)	616	330, 382	414
(2)	624	340, 384	397
(3)	606	330, 390	396
(4)	669	338 —	350
(5)	661	334 —	350

[a] Measured in methanol–ethanol (1 : 4 v/v). [b] Measured in Nujol mulls.

Table 5. E.s.r. parameters for the copper(II) complexes in methanol–ethanol (1 : 4 v/v) at 77 K

Complex	$10^4\lvert A_{\parallel}\rvert$/cm^{-1}	$g_{\parallel}$	$g_{\perp}$
(1)	150	2.28	2.07
	(149) [a]	(2.31) [a]	
(2)	153 [b]	2.28 [b]	2.08
(3)	147 [b]	2.28 [b]	2.08
(4)	180 [b]	2.29 [b]	2.07
(5)	132 [c]	2.24 [c]	2.09

[a] Minor species in parentheses. [b] Minor species were not well resolved, owing to weak intensities. [c] Only one species was observed.

also of the Cu^{II}S$_4$ type with only thioether as ligands ($g_{\parallel}$ = 2.09—2.12, $g_{\perp}$ = 2.03—2.04).[9] On the other hand, the $g_{\parallel}$ and $g_{\perp}$ values of the present complexes are compared with those of the Cu^{II}N$_4$ complexes involving only imidazole nitrogen donors [$g_{\parallel} = 2.26$, $g_{\perp} = 2.06$ for bis(2,2′-bi-imidazole)-copper(II) diperchlorate;[9] $g_{\parallel} = 2.26$, $g_{\perp} = 2.06$ for tetrakis(*N*-methylimidazole)copper(II) diperchlorate[9]], and of blue copper proteins ($g_{\parallel}$ = 2.19—2.30, $g_{\perp}$ = 2.05—2.08).[1] These results suggest that the co-ordination of imidazole ligands may increase the $g_{\parallel}$ and $g_{\perp}$ values of copper(II) complexes.

It has been reported that the increase of positive charges on the metal–ligand complex and the tetrahedral distortion of a planar Cu^{II}X$_4$ moiety cause the decrease of $\lvert A_{\parallel}\rvert$ and the increase of $g_{\parallel}$ values simultaneously.[9] In fact, the $g_{\parallel}$ value of the Cu^{II}N$_4$ as well as Cu^{II}S$_4$ complexes tends to increase as the $\lvert A_{\parallel}\rvert$ value decreases. Such a tendency, however, is vague in the Cu^{II}S$_2$N$_2$ complexes.[9] In the present complexes the $g_{\parallel}$ values appear to decrease with decreasing $\lvert A_{\parallel}\rvert$. The $\lvert A_{\parallel}\rvert$ values obtained for (1)—(3) and (5) are smaller than those of Cu^{II}S$_2$N$_2$ complexes with both amino- or pyridyl-nitrogen and thioether sulphur as ligating atoms (173×10^{-4} to 183×10^{-4} cm^{-1});[9] in particular, (5) exhibits a significantly small $\lvert A_{\parallel}\rvert$ value. This may be due to a distinct distortion of a square-planar configuration of the Cu^{II}S$_2$N$_2$ skeleton toward a tetrahedral geometry. Moreover, the powder e.s.r. spectrum of (5) at 77 K showed a weak signal due to a $\Delta M = \pm 2$ transition, indicating that (5) involves some metal–metal interaction in the solid state.

Electrochemical parameters of the copper(II) complexes (1)—(5) obtained by cyclic voltammetry are summarized in Table 6. The separations between anode and cathode peak potentials are 60—100 mV in methanol containing [NBu$^n_4$][BF$_4$] as a supporting electrolyte, although they are 100—300 mV when [NBu$^n_4$][ClO$_4$] is used in place of [NBu$^n_4$][BF$_4$]. In addition, the peak separations in methanol containing [NBu$^n_4$][BF$_4$] were almost independent of sweep rates (10—100 mV s^{-1}). Thus, the redox process for the copper(II) complexes is essentially reversible. This is confirmed also by the change of the electronic absorption spectra of (1) during the electrochemical reduction and the subsequent oxidation under a nitrogen atmosphere (see Figure 5); the sulphur–copper c.t. band around 380 nm decays on the controlled-potential reduction at +0.10 V *vs.* s.c.e., and is recovered completely on the subsequent oxidation at +0.50 V *vs.* s.c.e. A similar spectral change was observed in the redox reaction of (2)—(5) in methanol.

Table 6. Electrochemical parameters for the copper(II) complexes

Complex	$E_{\frac{1}{2}}$ [a]/V [NBu$^n_4$][BF$_4$] [b]	 [NBu$^n_4$][ClO$_4$] [b]
(1)	+0.33(60)	+0.28(110)
(2)	+0.37(85)	+0.35(300)
(3)	+0.34(60)	+0.30(130)
(4)	+0.36(100)	+0.32(100)
(5)	+0.23(65)	+0.23(140)

[a] $(E_{pc} - E_{pa})/2$ V *vs.* s.c.e. in methanol, calibrated with $E_{\frac{1}{2}}$ of ferrocene/ferrocenium cation (+0.328 V *vs.* s.c.e.; J. W. Diggle and A. J. Parker, *Electrochim. Acta*, 1973, **18**, 975); sweep rate 0.1 V s^{-1}; $\lvert E_{pc} - E_{pa}\rvert$/mV in parentheses. [b] Supporting electrolyte (0.1 mol dm^{-3}).

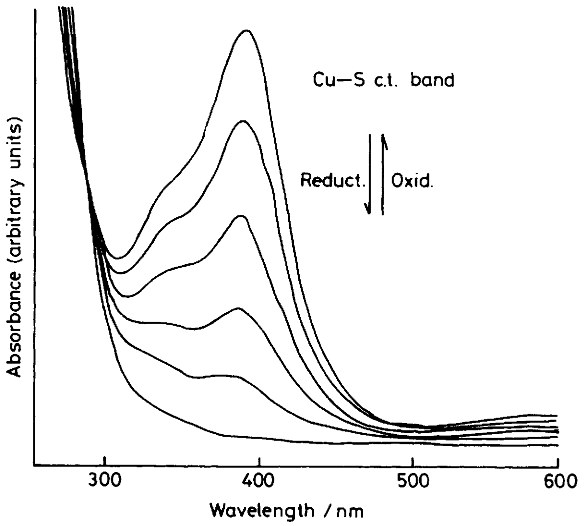

Figure 5. Changes of the electronic absorption spectra of [Cu(L^1)$_2$][ClO$_4$]$_2$ (1) during the electrochemical reduction and the subsequent oxidation in methanol containing [NBu$^n_4$][BF$_4$] (0.1 mol dm^{-3}) as a supporting electrolyte at 25 °C

The $E_{\frac{1}{2}}$ values obtained for the present complexes (+0.23 to +0.37 V *vs.* s.c.e.) are higher than those not only of the Cu^{II}N$_4$ complexes such as various bis(*N*-substituted pyrrole-2-carboxaldiminato)copper(II) (−1.0 to −0.4 V *vs.* s.c.e.)[26] but also of the Cu^{II}S$_2$N$_2$ complexes such as 2,10-diamino-4,8-dithiaundecanecopper(II) diperchlorate (−0.06 V *vs.* s.c.e.),[9] whereas they are somewhat smaller than the $E_{\frac{1}{2}}$ values of copper(II) complexes with bis(pyridyl)- and dithioether-containing tetradentate ligands (+0.47 to +0.65 V *vs.* s.c.e.).[6] Thus, it should be mentioned that the $E_{\frac{1}{2}}$ values of (1)—(5) are comparable with those of blue copper proteins (0 to +0.6 V *vs.* s.c.e.).[1]

Kinetics of the Reduction of the Copper(II) *Complexes with Ferrocene*.—When a methanol solution of (1) was mixed with ferrocene (fc) in the same solvent, the band at 382 nm due to the sulphur–copper c.t. transition weakened in its intensity and the concomitant appearance of a band due to the ferrocenium cation (fc$^+$) centred at 619 nm was observed, indicating the

Table 7. Pesudo-first-order rate constants for the electron-transfer reaction between $[Cu(L^1)_2]^{2+}$ and ferrocene in methanol containing $[NBu^n_4][BF_4]$ (0.1 mol dm^{-3})

T/°C	$10^4[Cu(L^1)_2{}^{2+}]$/ mol dm^{-3}	10^3[fc]/ mol dm^{-3}	$k_{obs.}$*/ s^{-1}
11.3	4.36	4.49	4.11
		6.73	5.89
		11.2	8.10
		16.8	9.58
		22.4	13.3
17.6	4.36	4.49	6.18
		6.73	8.90
		11.2	12.4
		16.8	15.5
		22.4	20.9
23.5	4.36	4.49	11.1
		6.73	17.5
		11.2	23.0
		16.8	29.8
		22.4	39.0
29.6	4.36	4.49	16.2
		6.73	24.1
		11.2	34.0
		16.8	44.0
		22.4	63.8

* The reproducibility is within ±5%.

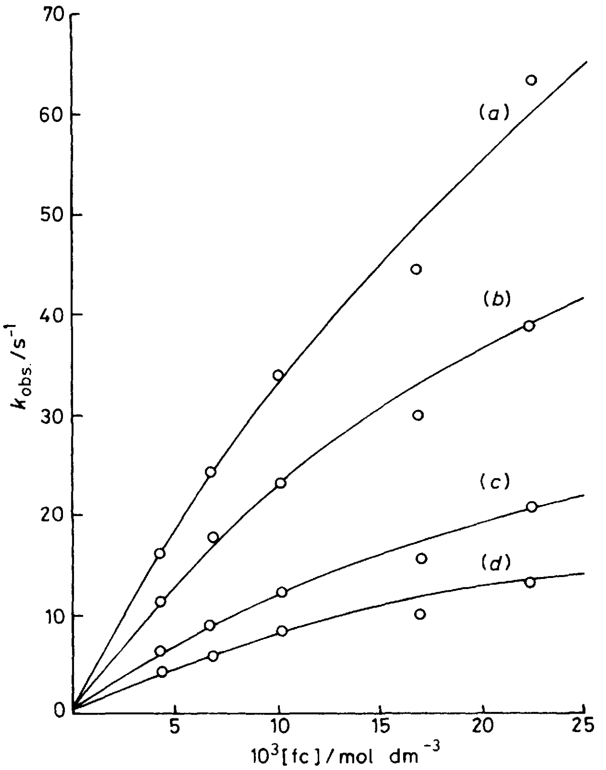

Figure 6. Plots of $k_{obs.}$ against [fc] for the reaction of $[Cu(L^1)_2]^{2+}$ with ferrocene at (*a*) 29.6, (*b*) 23.5, (*c*) 17.6, and (*d*) 11.3 °C

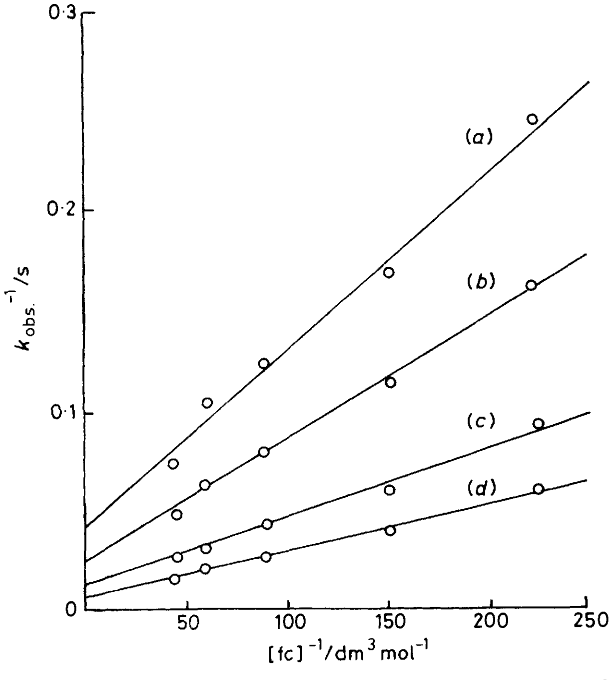

Figure 7. Plots of $k_{obs.}^{-1}$ against $[fc]^{-1}$ for the reaction of $[Cu(L^1)_2]^{2+}$ with ferrocene at (*a*) 11.3, (*b*) 17.6, (*c*) 23.5, and (*d*) 29.6 °C

$$[Cu(L^1)_2]^{2+} + fc \xrightarrow{k_{obs.}} [Cu(L^1)_2]^{+} + fc^{+} \qquad (i)$$
$$(1;\ R = Pr^n)$$

occurrence of the redox reaction shown in equation (i). Plots of $\log|A_t - A_\infty|$ *vs.* time, where A_t and A_∞ are absorbances at 382 nm at a time t and at the end of the reaction respectively, showed a good linearity for at least three half-lives, from which pseudo-first-order rate constants, $k_{obs.}$, were calculated. The $k_{obs.}$ values at four different temperatures are listed in Table 7. If one assumes that the reaction proceeds *via* two successive steps (the formation of a precursor complex followed by the electron-transfer process), the reaction of (1) with ferrocene can be expressed as equations (ii) and (iii), where $[Cu{\cdot}fc]^{2+}$

$$[Cu(L^1)_2]^{2+} + fc \overset{K}{\rightleftharpoons} [Cu{\cdot}fc]^{2+} \qquad (ii)$$
$$(1;\ R = Pr^n)$$

$$[Cu{\cdot}fc]^{2+} \xrightarrow{k_{et}} [Cu(L^1)_2]^{+} + fc^{+} \qquad (iii)$$

represents the precursor complex, K is the equilibrium constant of equation (ii) and k_{et} is the rate constant for the electron transfer reaction [equation (iii)]. According to this scheme, the $k_{obs.}$ value in the presence of a large excess of ferrocene can be expressed by equation (iv). If $K[fc] \ll 1$ ([fc] = the concentration of ferrocene), that is, K is sufficiently small, equation (iv) is reduced to $k_{obs.} = k_{et}K[fc]$, which predicts a linear dependence of $k_{obs.}$ on [fc]. In the reaction of (1) with ferrocene, however, there exists no linear relation between those quantities, as depicted in Figure 6. On the other hand, equation (iv) is transformed to equation (v), which predicts a linear relationship between $k_{obs.}^{-1}$ and $[fc]^{-1}$. This is confirmed to be valid as shown in Figure 7. The k_{et} and K values can be obtained from the intercepts and the slopes, respectively, of the straight line in Figure 7. The kinetic parameters for the reactions of (2), (3), and (5) with ferrocene were similarly de-

$$k_{obs.} = \frac{k_{et}K[fc]}{1 + K[fc]} \qquad (iv)$$

$$\frac{1}{k_{obs.}} = \frac{1}{k_{et}K[fc]} + \frac{1}{k_{et}} \qquad (v)$$

Table 8. Thermodynamic and activation parameters [a] for the reactions of the copper(II) complexes with ferrocene [b]

Complex	K/dm^3 mol^{-1}	$\Delta H^\ominus$/kJ mol^{-1}	$\Delta S^\ominus$/J K^{-1} mol^{-1}	k_{et}/s^{-1}	$\Delta H_{et}^\ddagger$/kJ mol^{-1}	$\Delta S_{et}^\ddagger$/J K^{-1} mol^{-1}
(1)	26.5 ± 2.7	−25 ± 1	−56 ± 4	109 ± 11	+73 ± 4	+38 ± 2
(2)	11.5 ± 4.8	−20 ± 1	−47 ± 2	402 ± 78	+77 ± 1	+64 ± 2
(3)	22.2 ± 5.2	−12 ± 1	−16 ± 1	149 ± 32	+82 ± 6	+71 ± 20
(4)	9.7 ± 2.3	−18 ± 2	−41 ± 1	327 ± 41	+68 ± 4	+33 ± 3
(5)	32.2 ± 3.3	−40 ± 2	−100 ± 6	18 ± 2	+78 ± 2	+42 ± 5

[a] Errors quoted are standard deviations. [b] In methanol containing 0.1 mol dm^{-3} [NBu$^n_4$][BF$_4$] at 25 °C.

Table 9. First-order rate constants for the reaction of $[\mathrm{Cu(L^1)_2}]^{2+}$ with ferrocene in methanol containing 0.1 mmol dm^{-3} [NBu$^n_4$][BF$_4$] at 4.7 °C; [fc] = 8.4 × 10^{-5} mol dm^{-3}

[Cu^{II}]/mol dm^{-3}	$k_{obs.}$/s^{-1}
8.40 × 10^{-4}	0.533 ± 0.02
1.40 × 10^{-3}	0.869 ± 0.01
2.10 × 10^{-3}	1.08 ± 0.02
2.80 × 10^{-3}	1.29 ± 0.03
4.20 × 10^{-3}	1.72 ± 0.02

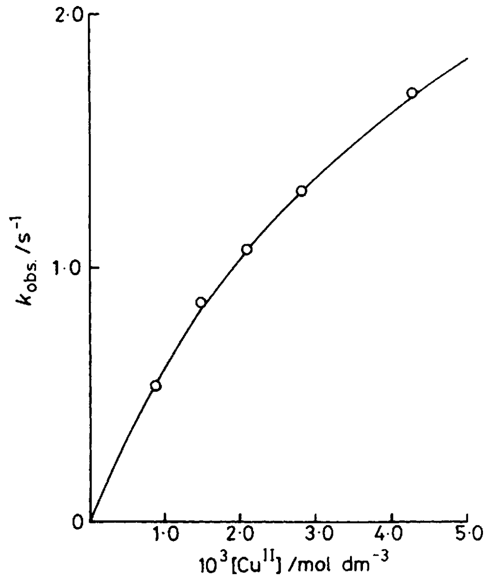

Figure 8. Plot of $k_{obs.}$ against [Cu^{II}] for the reaction of $[\mathrm{Cu(L^1)_2}]^{2+}$ with ferrocene at 4.7 °C; [fc] = 8.4 × 10^{-5} mol dm^{-3}

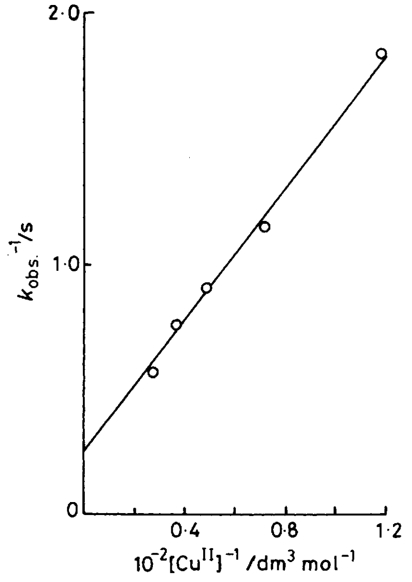

Figure 9. Plot of $k_{obs.}^{-1}$ against [Cu^{II}]$^{-1}$ for the reaction of $[\mathrm{Cu(L^1)_2}]^{2+}$ with ferrocene at 4.7 °C; [fc] = 8.4 × 10^{-5} mol dm^{-3}

termined, while those for the reaction of (4) with ferrocene were obtained by monitoring the increase of the absorbance at 275 nm due to the formation of the Cu^{I} species. The K and k_{et} values thus obtained are summarized in Table 8 together with thermodynamic and activation parameters calculated from K and k_{et} at four different temperatures. The values of K (9.7—32.2 dm^3 mol^{-1}) obtained here are consistent with the fact that K[fc] cannot be neglected in equation (iv).

Another possible mechanism may be considered: the copper(II) species reacts with ferrocene without the formation of a precursor complex [equations (vi) and (vii)], as reported for a redox reaction of bis{2,9-dimethyl-4,7-bis[(sulphonyloxy)-phenyl]-1,10-phenanthroline}copper(II) diperchlorate with sodium hexacyanoferrate(II) in water,[27] where Cu^{II} represents

$$\mathrm{Cu^{II}} \underset{k_{-1}}{\overset{k_1}{\rightleftharpoons}} \mathrm{Cu^{II*}} \qquad \text{(vi)}$$

$$\mathrm{Cu^{II*}} + \mathrm{fc} \xrightarrow{k_{et}} \mathrm{Cu^{I}} + \mathrm{fc^+} \qquad \text{(vii)}$$

a solvated copper species and Cu^{II*} a desolvated and active species. This mechanism predicts a linear relation between the $k_{obs.}$ value and the concentration of the Cu^{II} complex in the presence of an excess amount of the Cu^{II} species [equation (viii)]. The reaction with fc, however, indicates no linear

$$k_{obs.} = \frac{k_1 k_{et}[\mathrm{Cu^{II}}]}{k_{-1}} \qquad \text{(viii)}$$

relation between these quantities under the condition of using excess amounts of the Cu^{II} species (Table 9 and Figure 8). Moreover, plots of $k_{obs.}^{-1}$ against [Cu^{II}]$^{-1}$ are linear and give an intercept (Figure 9). These findings support the mechanism of equations (ii) and (iii).

The present copper(II) complexes have high electron-withdrawing properties as demonstrated by the high redox potentials. On the other hand, ferrocene has been reported to act as an electron donor toward π-acceptors such as *sym*-trinitrobenzene and tetracyanoethylene.[28,29] Thus, ferrocene may interact with the copper(II) complexes to form a precursor complex of the c.t. type prior to electron transfer. The negative $\Delta H^\ominus$ and $\Delta S^\ominus$ values are compatible with the formation of precursor complexes (Table 8). Although there have been reported several studies on the electron-transfer reactions of some copper(II) complexes with other metal complexes,[8,27,30,31] the formation of precursor complexes has never been presented. The electron-transfer reactions of blue copper proteins with some metal complexes were suggested to proceed *via* precursor complexes, which involve the interaction between the metal complexes and the histidine residue coordinated to the copper ion as the active site of blue copper proteins.[32–35] Thus, the redox reactions of the present copper(II) complexes with ferrocene may be similar to those of blue copper proteins with metal complexes as reductants.

The k_{et} value obtained increases with increasing redox potential of the copper(II) complexes. Moreover, the $\Delta S_{\text{et}}^{\ddagger}$ values are positively large for all the present reactions. This may largely be due to desolvation in a transition state of the reduction of the copper(II) complexes [equation (iii)], which accompanies the configurational change from tetragonal to tetrahedral geometry.

Acknowledgements

We thank Professor K. Nakatsu of Kwansei Gakuin University, Nishinomiya, for the use of the *X*-ray diffractometer and the programs for the structure solution and refinement.

References

1 R. Malkin and B. G. Malmström, *Adv. Enzymol.*, 1970, **33**, 177.
2 P. M. Colman, H. C. Freeman, J. M. Guss, M. Murata, J. A. M. Ramshaw, V. A. Norris, and M. P. Venkatappa, *Nature (London)*, 1978, **272**, 319; E. T. Adman, R. E. Stenkamp, L. C. Sieker, and L. H. Jensen, *J. Mol. Biol.*, 1978, **123**, 35.
3 C. C. Ou, V. M. Miskowski, R. A. Lalancette, J. A. Potenza, and H. J. Schugar, *Inorg. Chem.*, 1976, **15**, 3175.
4 K. D. Karlin, P. L. Dahlstrom, J. R. Hyde, and J. Zubieta, *J. Chem. Soc., Chem. Commun.*, 1980, 906.
5 G. R. Brubaker, J. N. Brown, M. K. Yoo, R. A. Kinsey, T. M. Kutchan, and E. A. Mottel, *Inorg. Chem.*, 1979, **18**, 299.
6 D. E. Nikles, M. J. Powers, and F. L. Urbach, *Inorg. Chim. Acta*, 1979, **37**, L499.
7 A. R. Amundsen, J. Whelan, and B. Bosnich, *J. Am. Chem. Soc.*, 1977, **99**, 6730.
8 F. T. Greenaway, L. M. Brown, J. C. Dabrowiak, M. R. Thompson, and V. M. Day, *J. Am. Chem. Soc.*, 1980, **102**, 7782.
9 U. Sakaguchi and A. W. Addison, *J. Chem. Soc., Dalton Trans.*, 1979, 600.
10 J. S. Thompson, J. L. Zitmann, T. J. Marks, and J. A. Ibers, *Inorg. Chim. Acta*, 1980, **46**, L101.
11 M. A. Augustin, J. K. Yandell, A. W. Addison, and K. D. Karlin, *Inorg. Chim. Acta*, 1981, **55**, L35.
12 R. A. Turner, C. F. Huebner, and C. R. Schloz, *J. Am. Chem. Soc.*, 1949, **71**, 2801.
13 J. A. Riddick and E. E. Toops, jun., 'Technique of Organic Chemistry,' 2nd edn., Interscience, New York, 1955, vol. 1, p. 416.
14 'International Tables for *X*-Ray Crystallography,' Kynoch Press, Birmingham, 1974, vol. 4.
15 C. K. Johnson, ORTEP-II, report ORNL 5138, Oak Ridge National Laboratory, Tennessee, 1976.
16 B. J. Hathaway and D. E. Billing, *Coord. Chem. Rev.*, 1970, **5**, 143.
17 L. Pauling, 'The Nature of the Chemical Bond,' 3rd edn., Cornell University Press, Ithaca, New York, 1960, p. 246.
18 M. M. Olmstead, W. K. Musker, and R. M. Kessler, *Inorg. Chem.*, 1981, **20**, 151.
19 G. Fransson and B. K. S. Lundberg, *Acta Chem. Scand.*, 1972, **26**, 3969.
20 F. Akhtar, D. M. L. Goodgame, M. Goodgame, G. W. Rayner-Canham, and A. C. Skapski, *Chem. Commun.*, 1968, 1389.
21 H. J. Prochaska, W. F. Schwindinger, M. Schwartz, M. J. Burk, E. Bernarducci, R. A. Lalancette, J. A. Potenza, and H. J. Schugar, *J. Am. Chem. Soc.*, 1981, **103**, 3446.
22 L. P. Battaglia, A. B. Corradi, G. Marcotrigiano, L. Menabue, and G. C. Pellacani, *J. Chem. Soc., Dalton Trans.*, 1981, 8.
23 T. G. Fawcett, S. M. Rudich, B. H. Toby, R. A. Lalancette, J. A. Potenza, and H. J. Schugar, *Inorg. Chem.*, 1980, **19**, 940.
24 M. D. Glick, D. P. Gavel, L. L. Diaddario, and D. B. Rorabacher, *Inorg. Chem.*, 1976, **15**, 1190.
25 K. D. Karlin, P. L. Dahlstrom, M. L. Stanford, and J. Zubieta, *J. Chem. Soc., Chem. Commun.*, 1979, 465.
26 H. Yokoi and A. W. Addison, *Inorg. Chem.*, 1977, **16**, 1341.
27 N. Al-Shatti, A. G. Lappin, and A. G. Sykes, *Inorg. Chem.*, 1981, **20**, 1466.
28 O. W. Webster, W. Mahler, and R. E. Benson, *J. Am. Chem. Soc.*, 1962, **84**, 3678.
29 M. Rosenblum, R. W. Fish, and C. Bennett, *J. Am. Chem. Soc.*, 1964, **86**, 5166.
30 N. Al-Shatti, M. G. Segal, and A. G. Sykes, *J. Chem. Soc., Dalton Trans.*, 1977, 1766.
31 M. A. Augustin and J. K. Yandell, *Inorg. Chem.*, 1979, **18**, 577.
32 M. G. Segal and A. G. Sykes, *J. Am. Chem. Soc.*, 1978, **100**, 4585.
33 A. G. Lappin, M. G. Segal, D. C. Weatherburn, and A. G. Sykes, *J. Am. Chem. Soc.*, 1979, **101** 2297.
34 A. G. Lappin, M. G. Segal, D. C. Weatherburn, R. A. Henderson, and A. G. Sykes, *J. Am. Chem. Soc.*, 1979, **101**, 2302.
35 P. M. Handford, H. A. O. Hill, R. W. Lee, R. A. Henderson, and A. G. Sykes, *J. Inorg. Biochem.*, 1981, **13**, 83.

Received 6th September 1982; *Paper* 2/1539